

# MULTIPACTOR DISCHARGE IN THE PIP-II SUPERCONDUCTING SPOKE RESONATORS

P. Berutti, T.Khabiboulline, G.Romanov

Technical division, Fermilab, Batavia, Illinois

October, 2014

Proton Improvement Plan-II at Fermilab is a plan for improvements to the accelerator complex aimed at providing a beam power capability of at least 1 MW on target at the initiation of LBNE (Long Base Neutrino Experiment) operations. The central element of the PIP-II is a new 800 MeV superconducting linac, injecting into the existing Booster. Multipacting affects superconducting RF cavities in the entire range from high energy elliptical cavities to coaxial resonators for low-beta applications. This work is focused on multipacting study in the low-beta 325 MHz spoke cavities; namely SSR1 and SSR2, which are especially susceptible to the phenomena. The extensive simulations of multipacting in the cavities with updated material properties and comparison of the results with experimental data helped us to improve overall reliability and accuracy of these simulations. Our practical approach to the simulations is described in details. For SSR2, which has a high multipacting barrier right at the operating power level, some changes of the cavity shape to mitigate this harmful phenomenon are proposed.

## INTRODUCTION

Proton Improvement Plan-II [1] at Fermilab is a plan for improvements to the accelerator complex aimed at providing a beam power capability of at least 1 MW on target at the initiation of LBNE (Long Base Neutrino Experiment) operations. The central element of the PIP-II is a new 800 MeV superconducting linac, injecting into the existing Booster. The PIP-II 800 MeV linac is a derivative of the Project X Stage 1 design as described in the Project X Reference Design Report [2]. The configuration of the 800 MeV linac is shown in Fig.1. A room temperature (RT) section accelerates H<sup>-</sup> ions to 2.1 MeV and creates the desired bunch structure for injection into the superconducting (SC) linac. Five superconducting cavity types operating at three different frequencies are required for acceleration to 800 MeV.

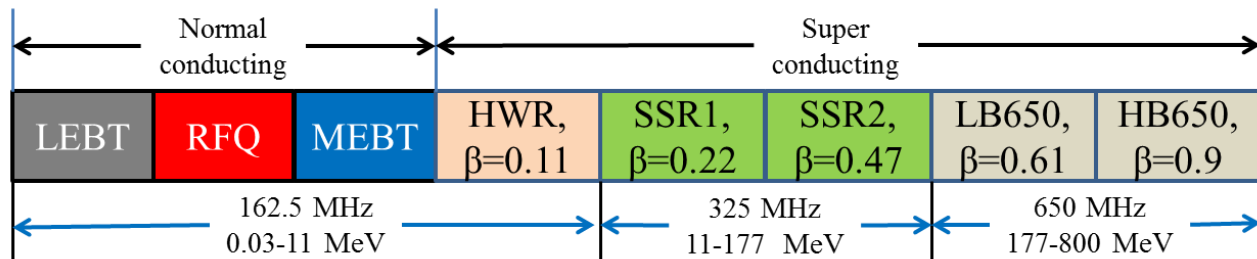


Figure 1: The PIP-II linac technological map.

The PIP-II linac includes the following major elements:

1. The room temperature (normal conducting) front-end, that consists of an ion source, LEBT, RFQ, and MEBT.
2. One superconducting accelerating section based on 162.5 MHz Half-Wave Resonators (HWR).
3. Two superconducting accelerating sections based on 325 MHz Single-Spoke Resonators (SSR1 and SSR2).
4. Two superconducting accelerating sections based on 650 MHz elliptical cavities (LB650 and HB650).

The electron multiplication on surfaces exposed to an oscillating electromagnetic field causes the phenomenon of multipacting, which can degrade significantly the performance of vacuum RF devices, especially accelerating cavities. It is a serious obstacle to be avoided for normal operation of particle accelerator and their RF components. In worst cases this phenomena, described in many accelerators, can completely prevent normal operation of an accelerating cavity. Multipacting affects superconducting RF cavities in the entire range from high energy elliptical cavities to coaxial resonators for low-beta applications. This work is focused on multipacting study in the low-beta structures; namely SSR1 and SSR2 (see Fig.2).

Multipacting (MP) seems to be a common problem for low beta SC spoke cavities. The high power tests of the first prototypes of SC spoke cavities [3] showed the signs of MP. Initially there was a tendency to explain the problems with RF conditioning by high field emission since the multipacting occurred in a broad interval of unusually high accelerating gradients of 2-5 MV/m [4]. Electron multipacting is a low field phenomena, and it was thought (basing on the experience with room temperature accelerating cavities) that it cannot exist at such high gradients. In fact there are regions in the spoke cavities where the electric field is low, compared to the accelerating gradient, and it combines with magnetic field in a way that provides conditions for electron multipacting in a broad interval of power levels. That was confirmed after new advanced computing capabilities made it possible to simulate particle dynamic in the realistic 3D electromagnetic fields, and first indications of multipacting in single spoke cavity were reported [5], though the existence of several levels of MP and its broad band character were not explained at that time.

The broad band character of the multipacting is very concerning issue for the SSR design. Multiple MP levels make RF conditioning longer and what is more importantly the MP barriers exist close or even exactly at the operating power level. The experience of Fermilab with MP in low-beta structure includes RF design, manufacturing and successful high power testing of 12 SSR1 cavities [6]. This experience combined with the extensive simulations of the multipacting [7, 8] provided clear understanding of the phenomena behaviour in the single spoke resonators.

Study of MP in SSR2 was a primary goal of this work along with sharpening of the simulation technique. SSR2 is a spoke resonator currently under development for PIP-II linac [9], it also operates at 325 MHz and its optimal beta is 0.47. The design has been finalized recently, and it was necessary to understand at what power level this resonator is affected by multipacting, what the critical accelerating gradients are, where the MP develops in the cavity volume and what can be done to mitigate this harmful phenomena.

## SIMULATION TECHNIQUE

### *General remarks*

A general approach for multipacting simulation was developed a while ago and it can be mapped to the three steps. These steps are performed in every case, with variations in execution, strategies for detailed implementation and

numerical methods. The first step is the definition of the geometry and the calculation of the RF and static fields in this geometry. In a second step, a motion of large number of particles is tracked in the structure. And in a third and final step a multipacting behaviour in the collection of particle tracking data is identified [10].

There are a number of numerical simulation codes for predicting multipactor, each with various pros and cons. Our choice is CST Studio Suite because all three steps are smoothly integrated in one package and because of its well-balanced features. CST PS combines flexible and developed modelling, electromagnetic field simulation, multi-particle tracking, adequate post-processing and advanced probabilistic emission model (Furman-Pivi model [11]), which is the most important new capability in the multipactor simulations. The emission model includes the stochastic properties of secondary emission in simulation and adds elastic and re-diffused reflection of primary electrons from the surfaces. The inclusion of the probabilistic factors of re-emission along with elastic scattering and re-diffusion broadens the multipactor bands and predicts the occurrence of multipactor well beyond “classic” model predictions [12, 13, 14].

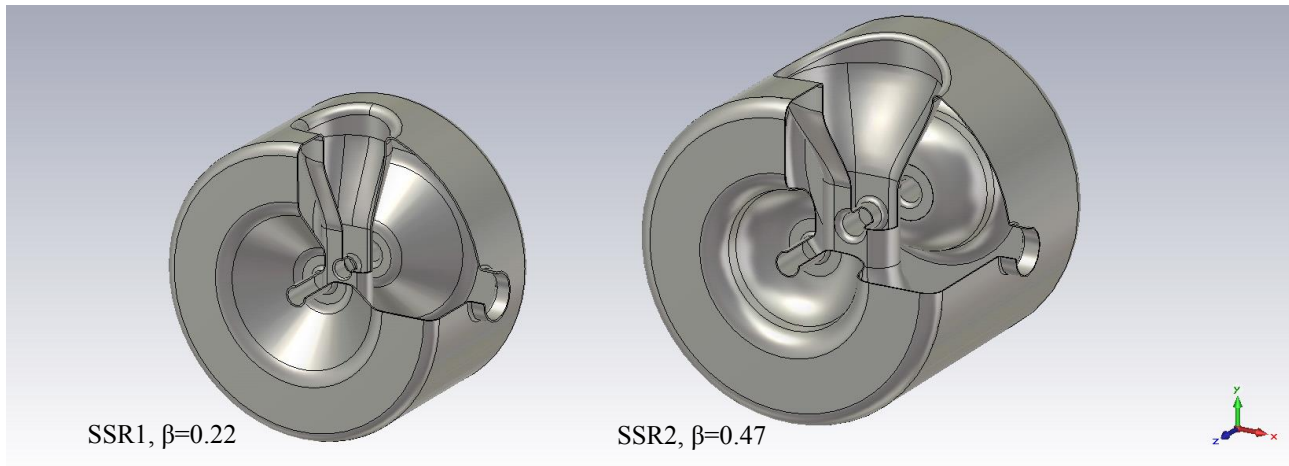


Figure 2: The models of SSR1 and SSR2

CST Studio Suite combines many special codes, but for MP simulations only few of them are needed: They are: CST MicroWave Studio (CST MWS) with eigenmode solver to calculate high frequency electromagnetic fields, CST Particle Studio (CST PS) with tracking and particle-in cell solvers to perform particle tracking, and CST Electromagnetic Studio (CST EM) with static solver to calculate static electric and magnetic fields. At introductory level CST PS with tracking solver only may be sufficient for MP study because the solver has its own in-built eigenmode and static solvers. This possibility is especially important taking into account that licenses for every solver are expensive and sold separately. But for comprehensive study of MP an access to all mentioned solvers is desirable.

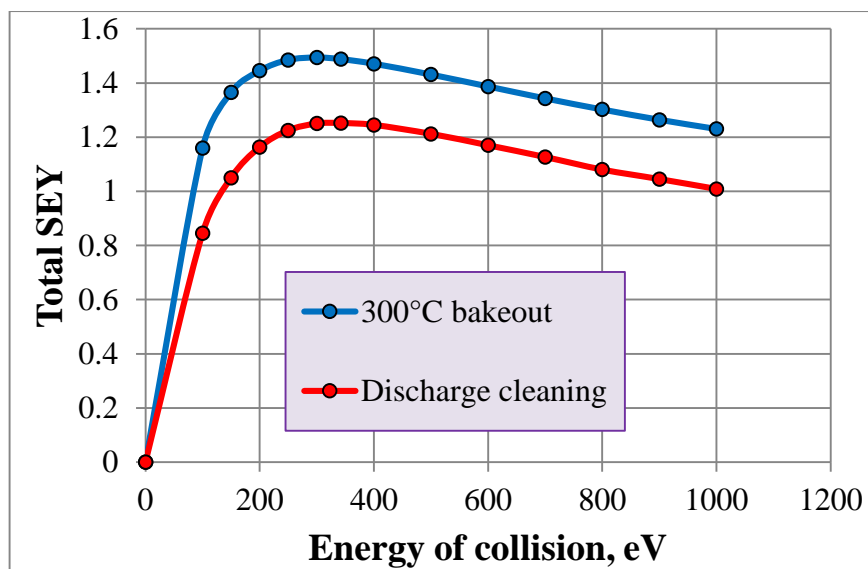


Figure 3: Total SEY of niobium used in the simulations.

CST PS offers two solvers for particle tracking; both can be used for MP simulations. One of them is the Gun Solver & Particle Tracking solver (TRK) which is used to compute trajectories of charged particles within RF fields and electrostatic or/and magnetostatic fields that can be calculated by in-built Eigenmode, Electrostatic and Magnetostatic solvers. The implemented gun-iteration enables the computation of a self-consistent electrostatic field which considers the reaction of the charged particle movement to the electrostatic potential distribution. Other one is the Particle-In-Cell solver (PIC) that computes the charged particles motion in self-consistent transient fields. This solver has in-built Transient solver, Electrostatic and Magnetostatic solvers. Usually the space charge effects are not taken into account in MP simulations, so just simple particle tracking in electromagnetic fields is used for both solvers in this work. The solvers are different by nature and have the specific parameters that will be discussed in separate paragraphs, where it is needed.

Besides accurate fields and particle tracking calculations, the developed library of emissive materials is highly critical. Currently in the CST PS material library there are three probabilistic emission models for niobium with different surface treatments: the wet treatment with the highest secondary emission yield (SEY), the 300°C bakeout with intermediate SEY and the argon discharge cleaned niobium surface with the lowest SEY. We assume that the high power tests of the cavities and their RF conditioning start with moderately clean cavity walls. Also we assume that when the nominal power level is reached and all MP barriers passed, then the cavity walls get additionally cleaned by MP and RF discharges with quality comparable to one of argon discharge cleaning. Therefore we performed MP simulations with the 300°C bakeout SEY model and with the discharge cleaned SEY model to evaluate MP parameters before and after RF conditioning. The total SEY curves (sum of true, elastic and re-diffusion secondary emissions) of both models are shown in Fig.3. It should be mentioned though, that the real SEY curves and their change during RF conditioning are not known.

### *Building a model for MP simulations*

**Solid modelling** in CST is quite advanced and allows to build very complex structures. Import of 2D and 3D CAD data in different formats is also available in case the engineering models are preferred. Typically a starting point of solid modelling for CST PS is the CST MWS solid models of the cavities built for the general design using eigenmode solver. Usually they are ready after RF design is done, so this part of model preparation is skipped - a detailed description of the solid modelling for MWS can be found elsewhere [15].

**Model preparation for TRK solver.** The CST MWS models are “vacuum” bodies embedded in the hidden background material with perfect electrical conductivity (PEC material, see Fig.4, a). These standard “vacuum” solid models from MWS cannot be used “as is” in PS, so the additional manipulations are needed. First of all, the models imported from MWS into PS have to be provided with metal walls. It is needed because the secondary emission properties in PS can be assigned to metal surface only (or saying more accurately - to a surface of any emissive material, like ceramic of vacuum window for instance), while PS does not recognize Perfect Electric Conductor background as a material body. A model with metal walls can be developed from scratch, but to avoid discrepancies between MWS and PS models it is more reliable and convenient to create the walls from “vacuum” models. It can be done using “Shell Solid” command from “Shape Tool” menu (see Fig.4,b). Then the material of the created walls is changed from initial “vacuum” to one with secondary emission properties (the materials with prefix SE in the CST material library). The walls should be reasonable thin to avoid problems with this conversion - thickness comparable to the smallest curvature radius in a model is recommended. In rare cases, when the “Shell Solid” command fails because of complex cavity geometry, then more robust “Fill up surrounding space” command from the same menu can be used instead. A resulting model is equivalent physically to a model with walls, it just looks less natural (see Fig.4,c). In both cases background material must be set to “Vacuum”.

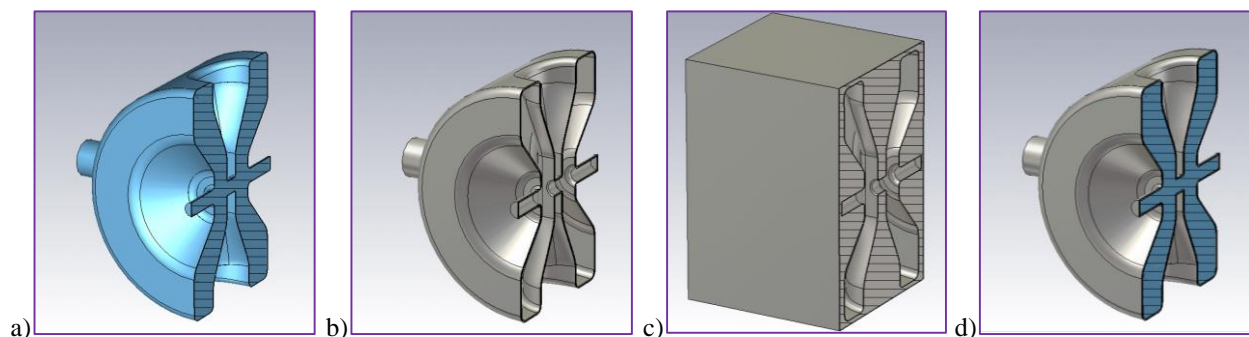


Figure 4: a) MWS “vacuum” model, b) PS model with metal walls, c) PS model with metal background, d) PS model with metal walls and vacuum body.

After the “Shell solid” command is applied a “vacuum” model disappears. If a single project is supposed to be used for both eigenmode and next following particle tracking simulations, then a copy of “vacuum” model must be created and

kept inside metal shell (see Fig.4,d). To eliminate parasitic modes outside cavity a material of background should be set to PEC. The steps of model preparation for both variants are given in Table 1.

Table 1

Step	Tracking only	Eigenmode + Tracking
1	Import MWS project model into PS	Import MWS model into PS
2	Create walls with “Shell Solid” command	Make a copy of “vacuum” model
3	Assign emissive material to the walls	Use one copy to create walls with “Shell Solid” command
4	Assign “vacuum” material to the background	Assign emissive material to the walls
5		Assign PEC material to the background

During post processing the secondary parameters of simulations are calculated for separate solids. So, it is useful to build a cavity model consisting of separate parts. It allows evaluating of MP on different surfaces independently.

**Model preparation for PIC solver.** The eigenmode solver is not incorporated into the PIC solver yet, so the external eigenmode RF electromagnetic fields have to be imported or simulated with built-in Transient solver. Simulation of RF fields with the built-in Transient solver is generally time consuming, so usage of this solver is justified only if the transient processes are really under interest. This is not our case, so only import of field maps is considered here. Therefore generally the model preparation for PIC solver could be the same as for “tracking only” mode of TRK. But there are two peculiarities of the PIC solver that change the routine procedure. One of them is a capability of the particles to “penetrate” by unknown reason the cavity walls and fly in the surrounding background vacuum. Of course this is a bug, which will be definitely fixed in future, but it was still there in 2014 version of CST PS. To avoid such “wild” particles we used the models consisting of vacuum RF body for particles to fly in, the walls with assigned SEY properties and PEC background which seals a cavity. The other feature is an essential one – time of simulation with PIC solver depends strongly on the total number of mesh cells. To reduce total number of meshcells and accordingly time of simulations, we decided to use 1/8 of the cavity models using geometrical symmetry planes. Boundary conditions at the planes of symmetry must provide mirror reflection of the particle trajectories to emulate particle motion in a full volume cavity. But there are no boundary conditions in CST PS that simulate mirror reflections of the electrons. So, we closed symmetry planes of the models with metal walls and assigned to them the emission properties with 100% reflection and zero true and diffusion secondary emission yield (see Fig.5). These walls do not simulate true mirror reflection since the angle of reflection is still random according to the Furman model, but at least they prevent losses of electrons and their energy. We also use 1/8 size models for TRK solver to reduce mesh cells number at given mesh density.

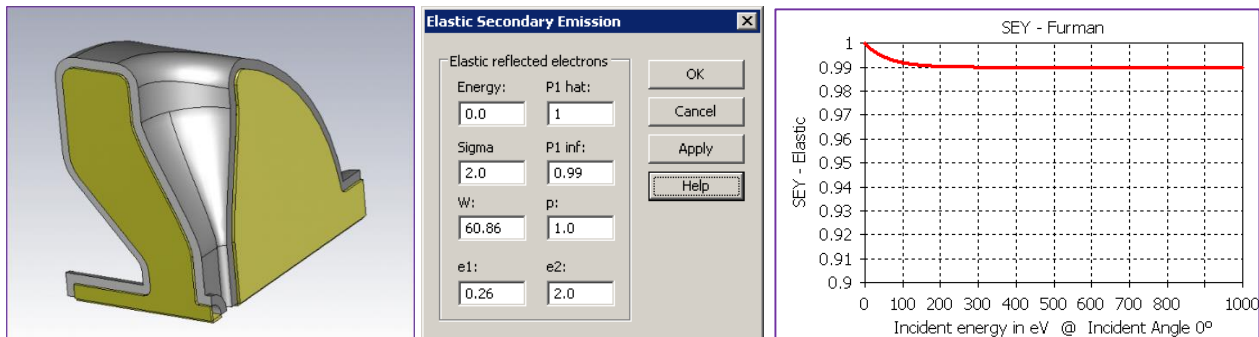


Figure 5: “Mirror” walls in 1/8 cavity model and setting for elastic scattering.

## Meshing

Both PIC and TRK solvers use only hexahedral mesh for tracking. As well both PIC and TRK solvers use hexahedral mesh for field calculation with their built-in electromagnetic solvers, if this option is chosen. Our preference for both solvers is to use imported field maps that were calculated separately with more effective tetrahedral mesh (available for eigenmode and frequency domain solvers). Multipacting is ultimately near surface process, so a possibility to enhance density of tetrahedral mesh near cavity surface, as shown in Fig.6, is very important. To create this mesh enhancement a cavity model for MWS is made consisting of two vacuum solids: outer layer of appropriate thickness (Shell Solid command is used) and internal body. Then the mesh density can be set for each body independently.

Hexahedral mesh for tracking does not have such flexibility –the mesh just should be as dense as possible (also shown in Fig.6). In this work typical number of meshcells was  $0.4 \div 0.5$  M for tetrahedral mesh and  $30 \div 50$  M for hexahedral mesh per 1/8 models.

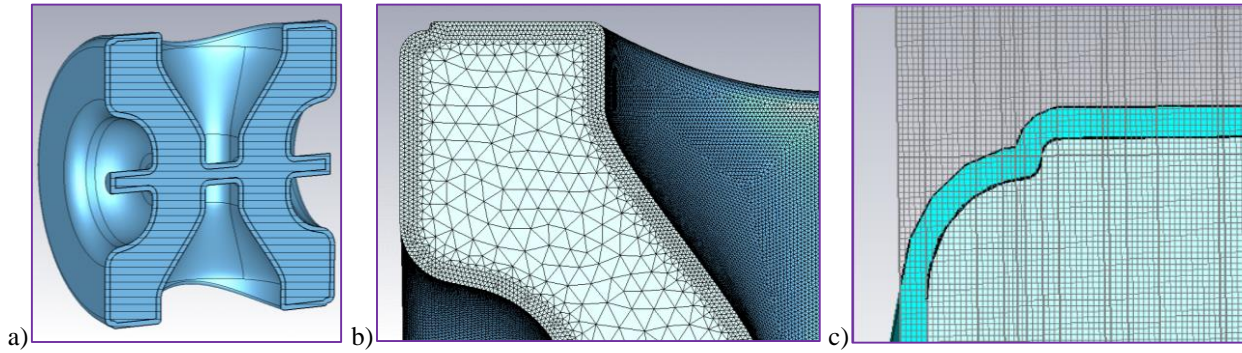


Figure 6: a) A cavity model consisting of two vacuum solids, b) tetrahedral mesh with enhanced density near wall surface for field simulations, 3) hexahedral mesh for particle tracking.

### Import of external field maps

In earlier versions of CST the import of external fields calculated with tetrahedral mesh into the tracking solvers that use hexahedral mesh was rather cumbersome. Now the procedure “Import from project” provides simple and fast field import from MWS to PS with minimal distortion of the original field distribution. Besides the imported fields are automatically cropped if only fraction of the models are used for MP simulations (1/8 model in our case).

During MP simulations particle tracking is performed many times at different electromagnetic field amplitudes and/or different particle source parameters without any other changes in the models. That means that the field distributions remain the same, and actually the same fields are used for tracking every time. Nevertheless, the tracking procedures in PS are organized in such a way that the electromagnetic fields are “prepared” every run, if they were imported, or they are simulated from scratch, if the built-in solvers are used. Of course, in both cases this is a waste of time and the fix was announced by CST for 2016 version. But currently, since “Field preparation” is much faster than the simulations using the built-in solvers, this is one more argument to use imported field maps.

### Indication of multipacting

The main characteristic of MP accelerating cavities is multipacting activity as a function of RF EM field level associated with acceleration rate. The field level may be expressed naturally as accelerating voltage  $V$  (magnitude of  $E_z$  integrated along cavity axis), effective voltage  $V_{\text{eff}}$  which takes into account transit time factor or energy gain of synchronous particle. In this paper the accelerating gradient defined as  $G = V_{\text{eff}}/\beta\lambda$  will be used as a field level parameter. The definition is rather conventional and applicable to the short one-three accelerating gaps cavities. But it is traditionally used for spoke cavity design and more importantly in the high power tests.

For indication of MP and evaluation of its probable intensity we use effective secondary emission yield  $\langle \text{SEY} \rangle$  and exponential growth rate coefficient  $\alpha$  that are defined and related as

$$\langle \text{SEY} \rangle = \frac{I_{\text{emission}}}{I_{\text{collision}}}; \quad N(t) = N_0 e^{\alpha t}; \quad \langle \text{SEY} \rangle = e^{\alpha T}.$$

Also energy of collision  $W_{\text{collision}}$  is useful to show where the field level is relatively to the maximum of material SEY:

$$W_{\text{collision}} (\text{eV}) = P_{\text{collision}} (\text{W}) / I_{\text{collision}} (\text{A}).$$

In these expressions  $t$  is time of simulation,  $T$  – RF period,  $N_0$  – initial number of particles; while current of emission  $I_{\text{emission}}$ , current of collision  $I_{\text{collision}}$  and power of collision  $P_{\text{collision}}$  are standard CST PS output averaged over last 3-5 RF periods to be used in the formulas. Obviously, that  $\langle \text{SEY} \rangle > 1$  and  $\alpha > 0$  indicate particle multiplication.

Typically growth of number of particles in MP simulations without space charge effects is exponential, but there are cases when it is not true, and the formulae above regarding  $\alpha$  are not correct. Effective secondary emission yield does not depend on character of particle number growth, therefore it is more robust and reliable indicator of MP.

In the earlier versions of CST effective secondary emission yield  $\langle \text{SEY} \rangle$  was defined as a ratio of number of secondary electrons to number of impacts. The latest versions of CST PS generate collision and emission currents instead of these numbers. In PIC solver macroparticles may have different charges, so the  $\langle \text{SEY} \rangle$  defined as a ratio of currents is not necessarily equivalent to the authentic one, defined through particle numbers. The difference is not essential for multipacting indication, but it should be kept in mind when comparison of multipacting intensities at different conditions

is performed. With respect to that the settings for initial particle current in PIC solver (particle source) should be chosen with some precautions, which will be described below.

### Particle sources in TRK solver and simulation.

TRK solver offers several types of particle sources including imported particles. Our typical choice is “Particle Area Source” with fixed emission model.

Properly defined particle source of initial electrons is extremely important for success and effectiveness of MP simulations in TRK. Theoretically a single electron emitted in right place at right moment can initiate multipacting, if MP exists and its parameters are known. But practically just more or less accurate guess can be done a priori about MP characteristic such as field level, type of multipacting, location, boundary of phase stability etc. (except very simple cases when all MP characteristics can be determined analytically). In fact these parameters is what should be found in the simulations.

Usually several locations in a cavity are suspicious as MP areas. TRK solver allows defining multiple particle sources, so they may be placed in every suspicious locations. Post-processing is performed separately for each particle source and for each separate solid body of a model as well. Therefore, it is useful to build a cavity model consisting of separate bodies and provide them with independent initial particle sources. Also the particle sources can be used in the simulations all at once or individually. All that helps to evaluate MP in different location independently and evaluate possibility of multipacting in each suspicious location.

The multiple particle sources should be used with caution. Particle source in TRK solver emits an instant single burst of electrons at default phase of imported RF field when simulation starts at time  $t = 0$ . The default phase of imported RF field is  $\varphi = 0^\circ$ , and it corresponds to maximal magnitude of RF electric field (time dependence  $\cos(\omega \cdot t + \varphi)$  is used in CST). But actual direction of the electric field relatively to particular emissive surface must be checked for every particle source, and the phase should be changed if needed to provide effective emission (see Fig.7). Since phase of initial emission is defined as a starting phase of imported RF field, it cannot be set for individual particle source, so all sources emit initial electrons simultaneously at the same phase. If some particle sources require different phases of field for initial emission, then they should be simulated separately by groups or one by one.

The initial electron emission on the crest of electric field is not effective for development of multipacting, because the default starting phase of  $0^\circ$  is outside of the intervals of phase stable motion at any field level. The most fast development of multipacting process would occur with initial emission at phases close to the synchronous phases, which are between  $-68^\circ$ – $(-115^\circ)$  for 2-point MP and between  $-20^\circ$ – $0^\circ$  for 1-point MP (exact values depends on level of field and average initial energy of secondary electrons) [16,17]. So, initial emission at  $-45^\circ$  is a good choice, since this phase is inside intervals of phase focusing almost in any case. In addition velocity spread of initial electrons, elastic and inelastic scattering distribute particles over phases and partially compensate fixed initial phase.

Number of the initial electrons is hard to define for each particular situation without trial runs. Generally it should be a compromise between simulation time and reliable results with solid statistical data. In the SSR1 and SSR2 models typical number of the initial electrons per particle source was 1–5 thousands.

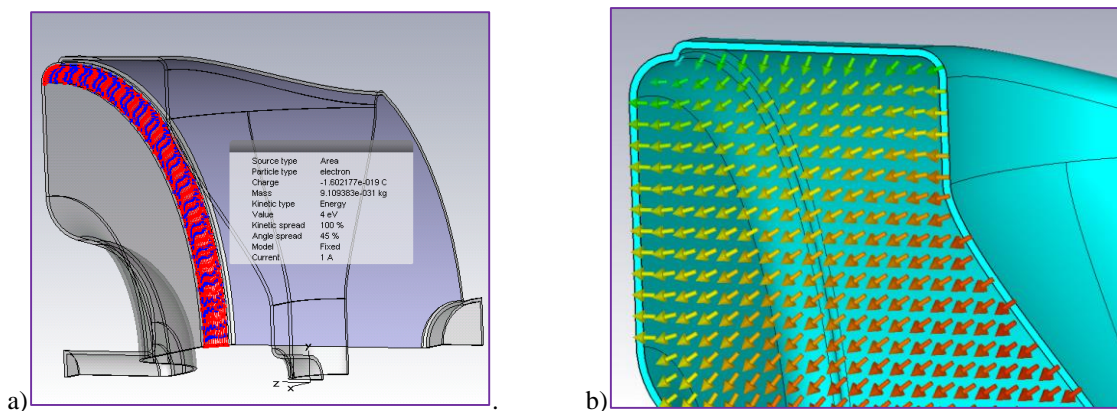


Figure 7: a) One of the particle sources. Red lines – surface triangulation, blue points – locations of the primary emission. b) “Positive” direction of electric field for given source of primary electrons.

### Particle sources in PIC solver and simulation.

In PIC solver the multiple particle sources also can be defined on different parts of the models. As opposed to TRK solver the sources cannot be used separately in PIC solver, and they emit altogether, though the parameters of emission for each particle source can be quite different. Post-processing does not recognize individual sources either, but it

calculates statistic data for each solid body separately. So, it is still useful to build a model consisting of separate parts and apply multiple particle sources.

The particle sources in PIC solver are time dependent. We use “Particle Area Source” with Gaussian emission model, which seems to be most flexible and convenient for MP simulations. The time dependence of the emission creates two problems that should be addressed.

First, Gaussian distribution refers to the emitting current, not number of particles. Each time step a user defined constant number of macroparticles are emitted from selected area of particle source. To make a generated pulse current of Gaussian shape, the solver assigns different charges to macroparticles. In other words, number of macroparticles is a linear function of time, while charge of macroparticles is a Gaussian function of time (see Fig.8). This may lead to an inconsistency with secondary emission model of material which deals with number of primary electrons and number of secondary ones. As a result of different charges of macroparticles the collision /re-emission currents may be nonequivalent to the numbers of secondary/primary electrons. Since CST PS post-processing does not calculate particle numbers any more, but only currents, this can create a confusion in estimation of MP intensity. With respect to that problem a pulse of initial particle current in PIC solver should be as close to rectangular shape as possible to avoid big difference in charges of macroparticles. Simply saying a value of  $\sigma$  of Gaussian function should be much bigger than particle emission pulse.

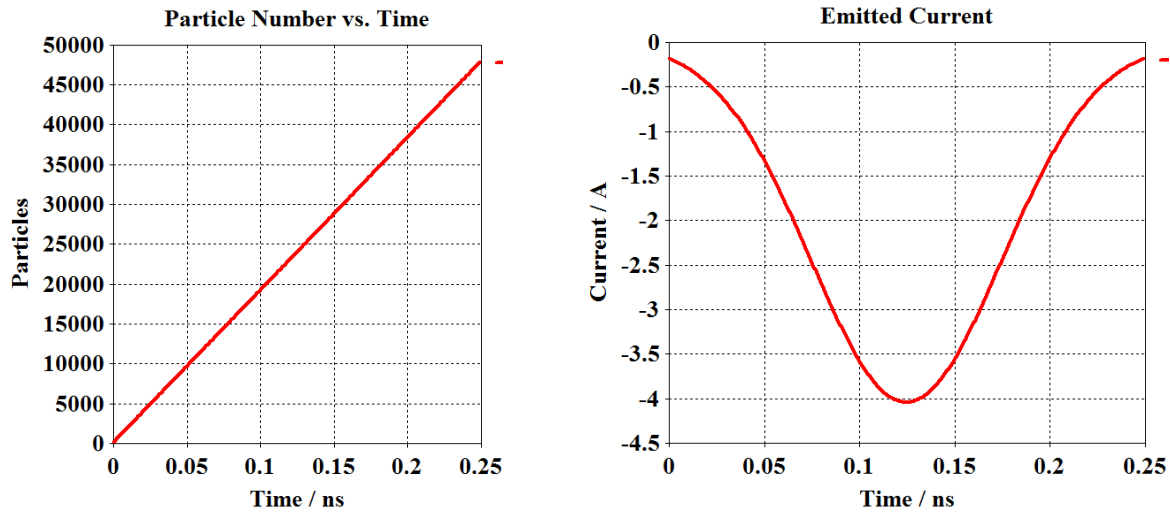


Figure 8: Number of particles and particle source current vs time of emission in Gaussian emission model.

Other problem is that a number of emitted particles depends on mesh size. Initial number of particles on selected face is defined by user (typically 100-300 in this work), then the source emits this number of particles every time step of integration, which in turn depends on the mesh size and on the required accuracy of integration. (It should be noted that the corresponding current pulse remains the same, which means that changing of mesh size also change charges of macroparticles) With dense mesh the number of electrons in the initial bunch becomes unnecessary large very quickly, and simulation time becomes unacceptably long. Therefore the choice is between high accuracy of simulations with dense mesh and reasonable time of simulation with risk to miss multipacting event because of poor accuracy. To resolve this dilemma several very short pulses of initial particles (bunches of particles) distributed over accelerating phases of RF electric field were used (see Fig.9). At any appropriate for re-emission field level at least one of bunches will be in the interval of stable phase motion.

We also tried Maxwellian particle source that is recommended by CST tutorials for MP simulations, but we did not find it effective or convenient.

### Comparison of the TRK and PIC solvers

Building of 3D models and calculation of the external electromagnetic fields are the same for both TRK and PIC solvers. The setting up of the solvers themselves for simulations requires approximately the same time and efforts. So, from preparation point of view the solvers are equal. Both solvers use the same secondary emission model, so the MP simulations basically are equivalent as well.

TRK solver calculates particle trajectories and that makes visual analyses of MP dynamic simple and easy. Multiple independent particle sources add convenience and flexibility to the simulations. TRK solver has in-built eigenmode, electro- and magnetostatic solvers, and that makes it a stand-alone application. In some cases this is a strong argument in favor of TRK.

The lack of any control on the simulation process must be mentioned among the “cons” of TRK solver in first place. It means that after TRK solver starts, a user does not have any possibility to check how a MP process is developing.

Consequently a user has either to wait until the solver performs all pre-defined number of time steps (often with huge number of particles close to the end of simulations) or interrupt a simulation run to check what is going on. Either way results in a waste of time. TRK solver is not very effective for indicating of non-resonant MP or MP with narrow interval of phase stability because of fixed initial phase. The solver often misses such events, this is a principal drawback that just has to be kept in mind. Post-processing also is not developed well enough. In general TRK solver potentially could be much faster and be more effective tool with appropriate upgrade. But currently PIC solver starts looking more preferable.

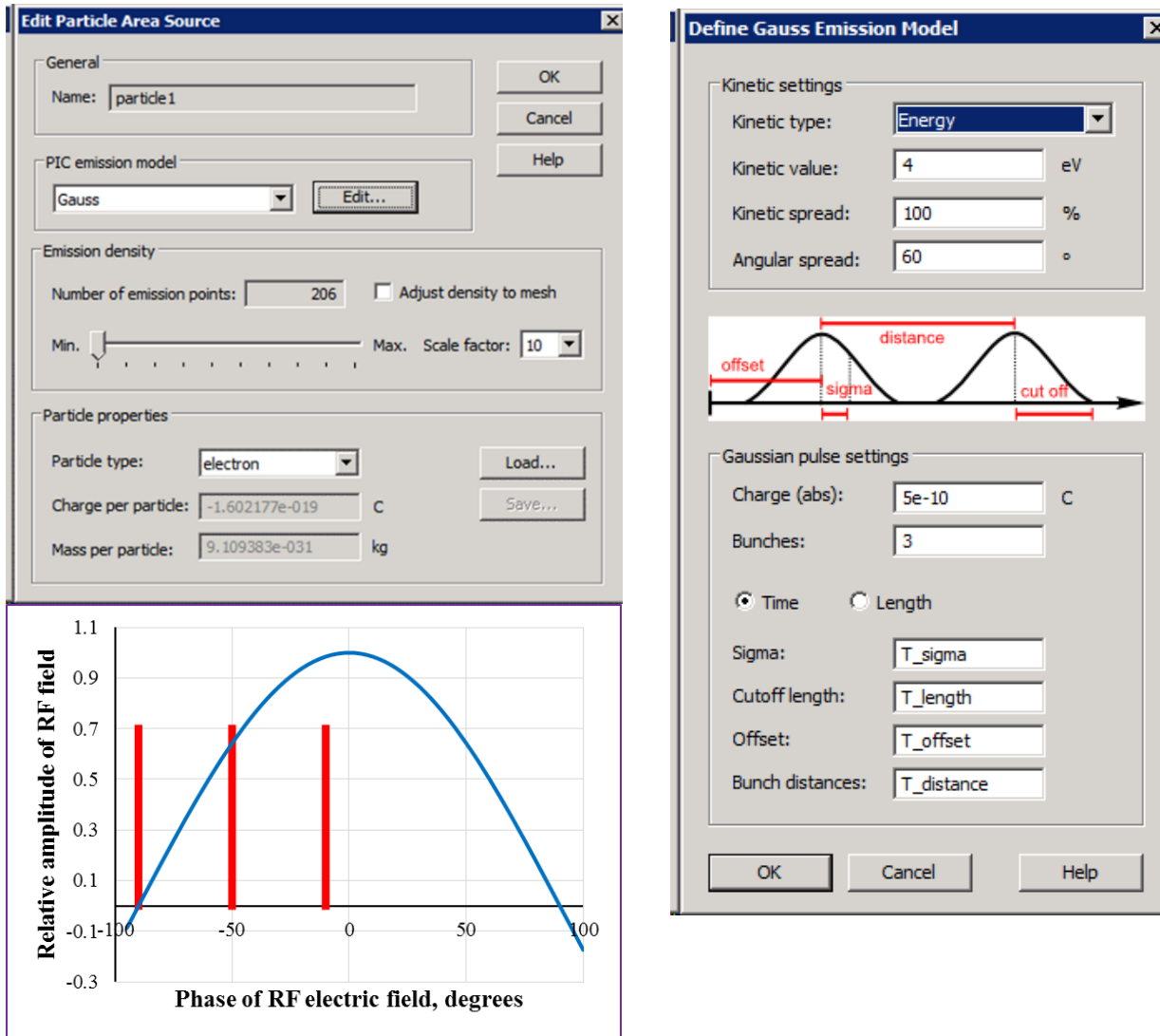


Figure 9: Settings for particle area source with Gaussian emission model.

PIC solver has several substantial advantages concerning MP simulations. Among them there are elaborated post-processing, time dependent emission of primary electrons, display of most important MP parameters in real time, i.e. on-line control of simulation process, and unique capability to take into account space charge effects which is a new trend in MP simulations. The solver, as it has been mentioned above, uses a single particle source only, this creates a serious inconvenience, of course. Also displaying of particle motion in form of trajectories would be useful too. Possible, but not absolutely indispensable, longer simulation time compared to TRK is a factor to consider, but due to the progress in computing capabilities it gradually becomes less and less important one.

## MP SIMULATION IN SSR1

Multipacting in the 325 MHz SSR1 cavity has been simulated already, and the results have been compared with experimental data on multipacting barriers found during the vertical test of the SSR1 cavity [18]. In this work the MP simulations in the SSR1 cavity were repeated because new secondary emission yield (SEY) data for niobium became available – the previous simulations of the SSR1 used SEY for copper, that allows defining RF power levels of MP, but is not sufficient to evaluate correct intensity and exact boundaries of MP discharge. More accurate simulations of MP in

SSR1 with updated material properties were important, because many SSR1 cavities were manufactured and tested at high power level, so the MP behaviour in SSR1 during RF conditioning is well known. Comparison of the simulations of MP in SSR1 with experimental data helped us to evaluate overall reliability and accuracy of these simulations.

To localize the areas of potential MP on the inner surface of the SSR1 the upper and lower limits of RF electric field levels  $E_{min}$  and  $E_{max}$  were defined in accordance with [19]. Only in this interval of field strength the electrons can gain proper incident energies that provide secondary electron emission sufficient for particle multiplication. The areas with corresponding surface electric field are shown at different accelerating gradients in Fig.10 (this is a quite accurate approximation since MP is a near surface process). It can be seen that the areas occupy a good portion of the cavity inner surface and exist from very low fields up to nominal accelerating gradient of 12 MV/m.

The multipacting spots appear locally only in the separate places of potential areas, because dynamic conditions for multipacting are not fulfilled everywhere at any given field level. In fact as the extensive simulations with CST Particle Studio show the most intensive spot of multipacting migrates from location to location with accelerating gradient increase (see Fig 11). While moving to the new areas the MP sees “fresh” unconditioned parts of the surface. This migration of MP location is the second reason for the broad interval of multipacting.

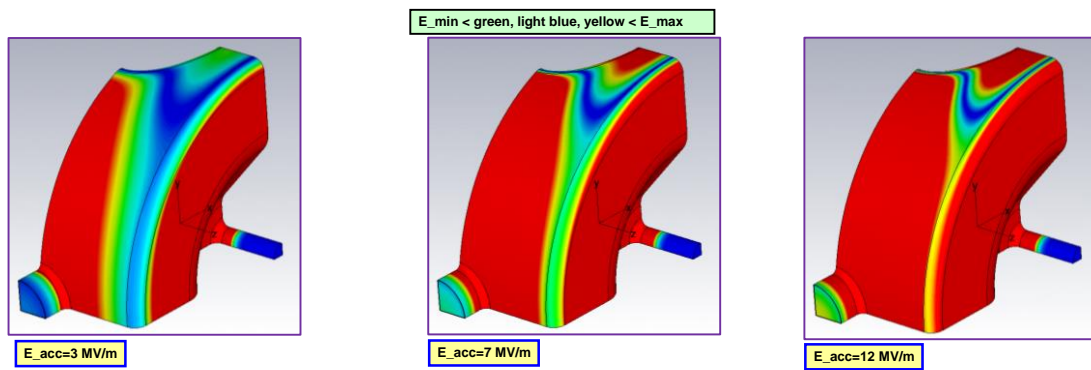


Figure 10: RF electric surface field distribution at different accelerating gradients. The areas in red and dark blue correspond to the field levels that are outside interval of  $E_{max} \div E_{min}$  and are free of multipacting.

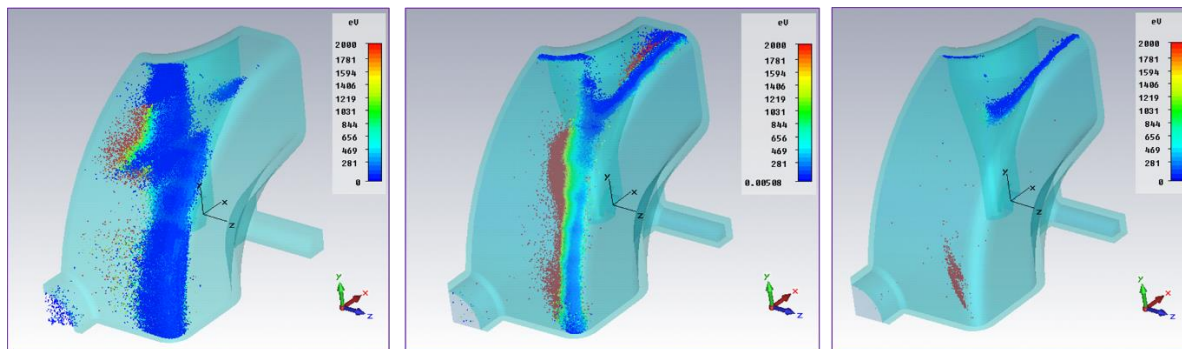


Figure 11: Particle distributions of MP at different accelerating gradients associated with the barriers.

Due to the vast areas of existence with variable field distributions the multipacting in SSR1 is always a mix of different particle dynamics modes, namely, one point non-resonant, one-point resonant and two-point resonant multipacting. Each of the modes dominates at certain levels of RF fields. As a result we can see in practice and in the simulations three major barriers of multipacting (see Fig.3). The first barrier exists in accelerating gradient interval of  $\approx 0.9-3.5$  MV/m and is associated mostly with non-resonant multipacting, typically it can be passed quickly. The one-point resonant multipacting dominates in the second barrier that starts at  $\approx 4$  MV/m. This barrier is the most stubborn one and it takes up to 30 hours of RF conditioning to pass it through. The third barrier is dominated by two-point resonant multipacting in the cavity corners. This kind of multipacting is the most “effective” one, but due to the small area of development the total emission current is not very high and RF conditioning is somewhat easier than for the second barrier. The area with the conditions favourable for multipacting continue shrinking with increasing of RF fields and gradually the intensity of multipacting drops to zero. The simulations are in excellent agreement with the experimental statistic data (see Fig.12).

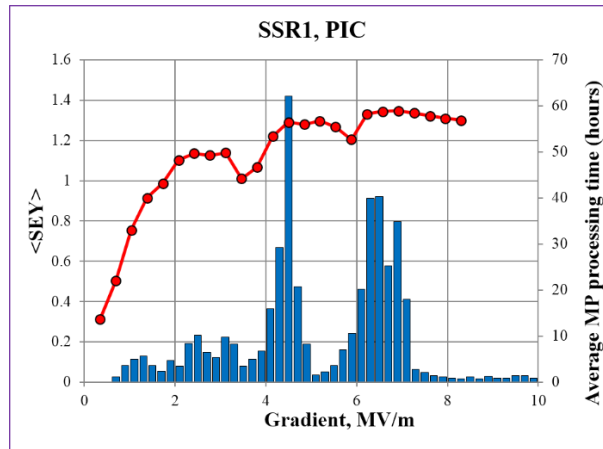


Figure 12: Effective secondary emission yield  $\langle \text{SEY} \rangle$  vs accelerating gradient as simulated with CST Particle Studio.  $\langle \text{SEY} \rangle$  greater than 1 indicates particle multiplication. The blue bars correspond to average processing time of SSR cavities required to get through the MP barriers.

### MP SIMULATION IN SSR2

Original design of SSR2 cavity showed high risk of multipacting – in simulations  $\langle \text{SEY} \rangle$  exceeds 1.2 in the broad interval of accelerating gradients even for discharge cleaned niobium [8]. Keeping in mind the very good agreement between simulations and practice for SSR1, we took this prediction seriously and decided to study different geometry changes to mitigate this phenomenon.



Figure 13: Proposed geometry change in SSR2 cavity (right) and original shape (left).

We studied a number of SSR2 geometry modifications trying to reduce risk of MP and keep the accelerating parameters intact at the same time. The simulations were performed with PIC and TRK solvers, using two different surface finish of material – baked niobium (higher SEY) and discharge cleaned niobium (lower SEY).

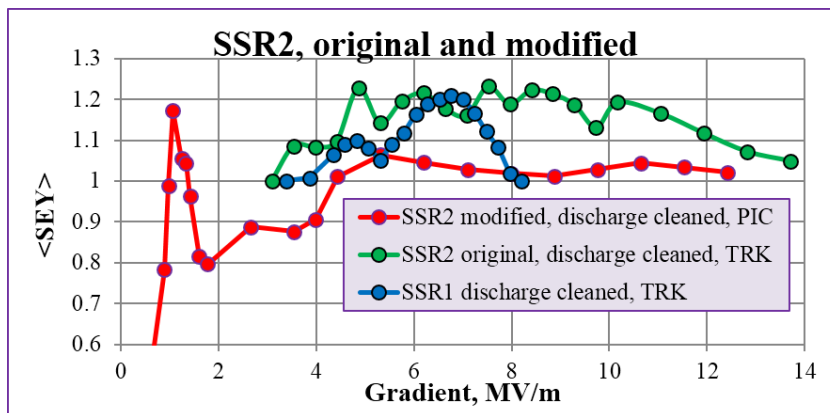


Figure 14: Reduced  $\langle \text{SEY} \rangle$  in modified SSR2 cavity compared to the original design and SSR1.

The most effective variant that we found includes double-radius corners (see Fig. 13). This main feature of the geometry does not actually suppress multipacting. It changes resonance conditions of MP, splitting main resonance and making overall process less intense and flattened (see Fig. 14). The result with discharge cleaned niobium is even better than for

SSR1 with the same surface treatment, which is encouraging fact, taking into account that we routinely achieve that level of surface finish in practice. No side effects that would degrade accelerating efficiency were found so far.

The simulations with different surface finish confirmed the conclusion made in [14] that the simulations with material with higher SEY are sufficient and preferable, because the simulating time is reduced since MP develops faster, and the simulations are more stable and consistent. The resulting  $\langle \text{SEY} \rangle$  curve for low emissive material would be similar and just accordingly lower (see Fig.15).

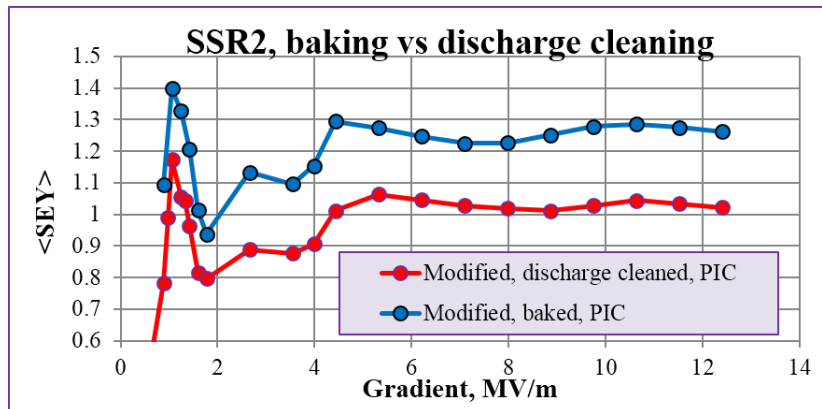


Figure 15: The simulations of MP in SSR2 with different surface treatment.

## CONCLUSION

New improvements in the simulation set up was described and discussed. It was shown that PIC and TRK solvers can deliver equivalent results. Also it was confirmed that the simulations with higher emissive materials are preferable for comprehensive and faster multipacting study

The simulations of multipacting in SSR1 with enhanced accuracy demonstrated very good agreement with experimental statistical data. The proposed geometry changes in SSR2 to mitigate intense multipacting were proved to be effective. Additional study will be conducted to avoid any possible side effects that could degrade cavity performance.

## REFERENCES

- [1] Proton Improvement Plan website, [http://www-ad.fnal.gov/proton/PIP/PIP\\_index.html](http://www-ad.fnal.gov/proton/PIP/PIP_index.html)
- [2] Project X Reference Design Report, S. D. Holmes (editor), arxiv: 1306.
- [3] K.W.Shepard et al, "Prototype 350 MHz Niobium Spoke-loaded Cavity". PAC'99, p. 955, New York, 1999.
- [4] T. Tajima et al, "Evaluation and Testing of a Low- $\beta$  Spoke Resonator", PAC'2001, Chicago, IL, 2001.
- [5] L.V.Kravchuk et al, Multipactoring Code for 3D Accelerating Structures, LINAC'00, Monterey, California, THB12, 2000.
- [6] L. Ristori et al, "Design, Fabrication and Testing of Single Spoke Resonators at Fermilab", SRF2009, Berlin, Germany, 2009
- [7] G. Romanov, "Simulation of Multipacting in HINS Accelerating Structures with CST Particle Studio", MOP043, Linac2008, Victoria, British Columbia, Canada, 2008
- [8] P. Berrutti et al, "Multipacting Simulations of SSR2 Cavity at FNAL",
- [9] M. Merio et al, "Update on SSR2 Cavities Design for Project X and Risp", WEPWO057, IPAC2013, Shanghai, China, 2013
- [10] F.L.Krawczyk, Status of Multipacting Simulation Capabilities for SCRF Applications, Proceedings of the 10th Workshop on RF Superconductivity, Tsukuba, Japan, 2001.
- [11] M.A. Furman and M.T.F. Pivi. "Probabilistic model for the simulation of secondary electron emission", Physical Review Special Topics, Accelerators and Beams, Volume 5. 2002.
- [12] R. Seviour, "The Role of Elastic and Inelastic Reflection in Multipactor Discharges", IEEE Trans. on Electron Devices, vol.54, No 8, August, 2005.
- [13] G.Romanov, "Stochastic Features of Multipactor in Coaxial Waveguides for Travelling and Standing Waves", Preprint FERMILAB-PUB-11-003-TD, 2011.
- [14] Gennady Romanov, "Update on Miltipactor in Coaxial Waveguides Using CST Particle Studio", PAC2011, New York, USA, 2011.
- [15] CST - Computer Simulation Technology, <https://www.cst.com/>
- [16] И.Н.Сливков, "Процессы при высоком напряжении в вакууме", Энергоатомиздат, Москва, 1986.

- [17] V.A.Puntus and G.V.Romanov, "Multipacting in the Phase Beam Monitor at MMF", EPAC98, WEP05D, June 1998, Stockholm, Sweden
- [18] I. Gonin et al., "High Gradient Tests of the HINS SSR1 Single Spoke Resonator", HB2008, Nashville, Tennessee, August, 2008.
- [19] В.Г.Мудролюбов, В.И.Петрушин, "Обобщённые соотношения для областей существования модификаций резонансного ВЧ разряда с учётом кулоновского поля", ЖТФ, т.XL, вып.5, май 1970, стр.1017.